

# Forced Response Prediction of Constrained and Unconstrained Structures Coupled Through Frictional Contacts

Ender Cigeroglu<sup>1</sup>  
e-mail: ender@metu.edu.tr

Ning An  
Chia-Hsiang Menq

Department of Mechanical Engineering,  
The Ohio State University,  
Columbus, OH 43210

*In this paper, a forced response prediction method for the analysis of constrained and unconstrained structures coupled through frictional contacts is presented. This type of frictional contact problem arises in vibration damping of turbine blades, in which dampers and blades constitute the unconstrained and constrained structures, respectively. The model of the unconstrained/free structure includes six rigid body modes and several elastic modes, the number of which depends on the excitation frequency. In other words, the motion of the free structure is not artificially constrained. When modeling the contact surfaces between the constrained and free structure, discrete contact points along with contact stiffnesses are distributed on the friction interfaces. At each contact point, contact stiffness is determined and employed in order to take into account the effects of higher frequency modes that are omitted in the dynamic analysis. Depending on the normal force acting on the contact interfaces, quasistatic contact analysis is initially employed to determine the contact area as well as the initial preload or gap at each contact point due to the normal load. A friction model is employed to determine the three-dimensional nonlinear contact forces, and the relationship between the contact forces and the relative motion is utilized by the harmonic balance method. As the relative motion is expressed as a modal superposition, the unknown variables, and thus the resulting nonlinear algebraic equations in the harmonic balance method, are in proportion to the number of modes employed. Therefore the number of contact points used is irrelevant. The developed method is applied to a bladed-disk system with wedge dampers where the dampers constitute the unconstrained structure, and the effects of normal load on the rigid body motion of the damper are investigated. It is shown that the effect of rotational motion is significant, particularly for the in-phase vibration modes. Moreover, the effect of partial slip in the forced response analysis and the effect of the number of harmonics employed by the harmonic balance method are examined. Finally, the prediction for a test case is compared with the test data to verify the developed method.*

[DOI: 10.1115/1.2940356]

## 1 Introduction

Mechanical systems with moving components always involve frictional contact, which appears in various applications such as turbine blades [1–10], mechanical joints [11–13], and clutches [14–16]. Due to the nonlinear nature of dry friction, dynamic analysis of structures constrained through frictional contacts is difficult. Several methods were developed in order to analyze these structures [1–16]; however, due to this difficulty, all of these methods were developed for specific cases such as shroud contact [9,10], bladed disks with wedge dampers [1–3,8], mechanical joints [11], and clutches [14,16]. Therefore, there is a need for a general approach for the analysis of structures constrained through frictional contacts.

In order to develop a general analysis method, one of the structures in the frictional contact is considered as unconstrained; therefore, it is constrained by the frictional contact and/or the geometric configuration only. This is a general case, which can

also handle friction contact between constrained structures. A typical example of frictional contact between constrained and unconstrained structures can be found in bladed-disk systems with blade-to-blade dampers [1–8], where the dampers move freely in between adjacent blades. In order to establish the developed forced response analysis method, in this study, a bladed-disk system with wedge dampers is used as an illustration in the rest of the paper. Here, blade and wedge damper constitute the constrained and unconstrained structures, respectively.

Wedge damper, unconstrained structure, is a widely used friction damper, which is also referred to as underplatform damper. It has two inclined surfaces on both sides and forced against the two neighboring blades by centrifugal forces. Due to the relative motion between the wedge damper and adjacent blades, the excessive energy of the blades is dissipated through frictional contacts. In order to increase the high cycle fatigue (HCF) life of turbine blades, optimal parameter values for the wedge damper and the bladed-disk system have to be determined, which can be achieved through a forced response analysis.

Yang and Menq [1,2] developed stick-slip contact kinematics for wedge dampers under two translational degrees of freedom. Authors developed analytical stick-slip transition criteria, including the variation of normal load, in order to simulate the stick-slip motion precisely. The harmonic balance method was used to predict forced response of bladed disk with wedge dampers, and an experimental test beam was analyzed and the simulation results

<sup>1</sup>Corresponding author. Present address: Middle East Technical University, Ankara, Turkey.

Contributed by the International Gas Turbine Institute of ASME for publication in the JOURNAL OF ENGINEERING FOR GAS TURBINES AND POWER. Manuscript received December 24, 2007; final manuscript received March 17, 2008; published online December 23, 2008. Review conducted by Patrick S. Keogh. Paper presented at the ASME Turbo Expo 2007: Land, Sea and Air (GT2007), Montreal, Canada, May 14–17, 2007.

were validated. A 3D wedge damper model with two-dimensional motion on the contact interface was developed by Sanliturk et al. [3]. A two-dimensional friction model for constant normal load was used, and the harmonic balance method is applied to predict forced response. A test case with two blades and a wedge damper was analyzed, and the results were compared with the simulations. In addition to wedge dampers, curved shape underplatform dampers were also studied by several researchers [4–7], and an underplatform damper with a curved and inclined surface was analyzed in Ref. [8]. All the models described above develop kinematic relations for the damper and blade, and the rigid body motion of the unconstrained structure is not modeled.

In order to determine nonlinear contact forces between two relatively moving bodies, different friction models can be utilized. In the analysis of friction damping, one-dimensional friction model was used widely [17–21]. This model is useful if the relative motion is one dimensional. It is possible to have planar motion, for which two-dimensional friction models are developed [22,23]. However, due to the interaction between two bodies, the normal load acting on contacting surfaces can vary with normal motion. Yang et al. [24] developed a one-dimensional friction model where the normal load was induced by the normal motions of the mating surfaces. Authors developed analytical transition criteria for stick-slip-separation transition and obtained analytical transition angles for simple harmonic motion. Normal load variation was also addressed by Yang and Menq [25] for three-dimensional motion (two-dimensional in-plane and one-dimensional out-of-plane motion) and by Chen and Menq [10] for three-dimensional periodic motion. Using similar criteria as developed in Ref. [24], Petrov and Ewins [26], for one-dimensional motion with normal load variation, later described an algorithm to determine transition angles numerically for periodic motion, similar to the one given in Ref. [27].

This paper presents a forced response prediction method for the analysis of constrained and unconstrained structures coupled through frictional contacts. The proposed model includes six rigid body modes and several elastic modes of the unconstrained structure; therefore, it may undergo three-dimensional translation and three-dimensional rotation, which are constrained by the friction contacts only. In the modeling of contact surfaces, discrete contact points associated with contact stiffnesses are distributed on friction interfaces. Contact stiffnesses at each contact point are determined by considering the effects of higher frequency modes, which are omitted in the dynamic analysis. The initial preload or gap at each contact pair varies with the normal force acting on the friction interface; therefore, a quasistatic contact analysis is performed initially in order to determine the contact area in addition to the initial preload or gap at each contact point due to the normal load.

In order to predict forced response of frictionally constrained structures, two-dimensional or three-dimensional friction models developed previously can be employed. However, in order to decrease computational time required for the forced response predictions, a simplified three-dimensional friction contact model based on the one-dimensional model with normal load variation [24] is proposed. In the proposed friction model, the three-dimensional relative motion on the contact surface is decomposed into two one-dimensional in-plane components and an out-of-plane component. The one-dimensional friction contact model is employed by assuming that these in-plane components are independent of each other. The harmonic balance method is used to represent the resulting nonlinear contact forces ensuing in a set of nonlinear algebraic equations. The relative motion at the contact surface is expressed by modal superposition; therefore, the number of unknowns resulting in the nonlinear equation set is only proportional to the number of modes used in the analysis. As a result, unlike receptance methods, the number of nonlinear equations is independent of the number of contact points used.

The developed method is applied to a tuned bladed-disk system

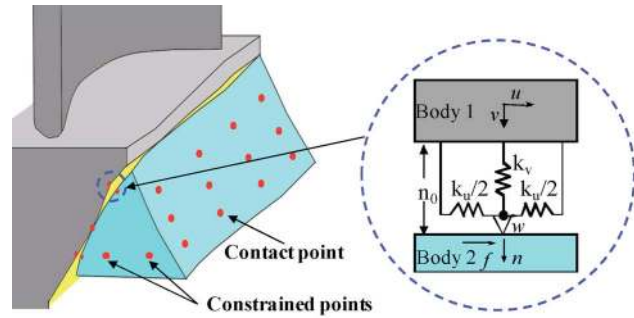


Fig. 1 Contact model for the wedge damper

with wedge dampers in order to obtain its forced response and optimal curves. In addition, the effects of normal load on the rigid body motion of the damper are studied. Specifically, the effect of the damper's rotational motion on the prediction of the forced response is analyzed. It is shown that the effect of rotational motion is significant, particularly for the in-phase vibration modes. The effect of partial slip in the forced response analysis is investigated. A blade-to-ground damper is studied in order to reveal the effects of multiple harmonics on forced response predictions. Finally, predictions for a test case are compared with available test data.

## 2 Model for Constrained and Unconstrained Structure

The forced response prediction method for constrained and unconstrained structures coupled through frictional contacts is presented on a bladed-disk system with wedge dampers, where the blade constitutes the constrained structure, and the damper constitutes the unconstrained structure. Accordingly, the motion of the damper is constrained by the frictional contacts and the geometric configuration of the damper between adjacent blades only. Consequently, the damper undergoes three-dimensional translation and three-dimensional rotation in addition to the elastic deformation. Elastic motion of the damper is necessary if the excitation frequency and/or static forces acting on the damper are high. However, with the proposed approach, it is possible to model the damper as completely rigid or rigid in certain directions and elastic in others by using the appropriate mode shapes.

**2.1 Contact Model.** The interaction between the blade and the wedge damper is modeled by discrete contact points evenly distributed on the two contact surfaces of the blade and damper. At each contact pair, contact stiffnesses in the three main directions of motion are determined in order to take into account the effects of higher frequency modes, which can be represented as residual stiffnesses. It is assumed that residual stiffnesses are only present between contact pairs; hence, they are called as contact stiffnesses. The determination of contact stiffnesses will be explained in the next section.

A blade and a wedge damper in contact are given in Fig. 1, where contact points represented by the dots are shown on the left, and contact stiffnesses between a contact pair in the local coordinate system are shown on the right. The contact points on the X-Y plane of the damper are called constrained points, which are used to constrain the motion of the damper in the Z direction due to space limitations, and it should be noted that the constrained force could be at most on one of the constrained planes. These constraints are due to the physical restrictions in real gas turbine engine, where the damper can move freely under the action of contact and centrifugal forces in a volume between the adjacent blades on the disk.

The motion of the blade and the wedge damper are expressed in the blade coordinate and damper coordinate systems, respectively. The coordinate systems for the  $i$ th blade and wedge damper are shown in Fig. 2. The blade coordinate system is on the rotary axis

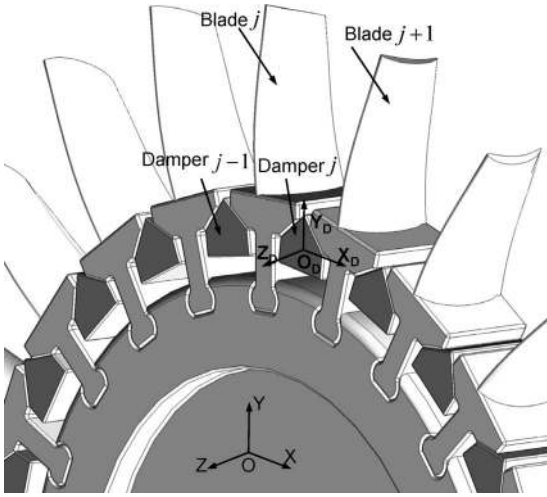


Fig. 2 Blade and damper coordinate systems

of the disk where the  $X$  and  $Y$  axes are coincident with the tangential and radial orientations of the  $i$ th blade, and the  $Z$  axis is determined by the right hand rule. The  $i$ th damper coordinate system is determined by three rotations about the blade coordinate axes. Coordinate systems for other blades and dampers can be obtained by a simple rotation about the  $Z$  axis with an amount of blade phase angle.

As shown in Fig. 3, wedge damper has four contact planes, where  $\alpha$  and  $\beta$  are used to define the orientations of the left and right contact planes. Coordinate systems for the front and the back constraint planes can be obtained by  $90^\circ$  and  $-90^\circ$  rotations about the  $X_D$  axis, and the coordinate systems for the right and the left contact planes can be obtained by  $-(90^\circ - \beta)$  and  $90^\circ - \alpha$  rotations about the  $Z_D$  axis. In Fig. 3 the coordinate system for the right plane is shown.

**2.2 Calculation of Contact Stiffness.** In the model proposed, in order to capture local deformation on the contact interface, very high frequency modes have to be included into the modal superposition approach, which is not practical in terms of calculation times. Therefore limited number of modes is used in the modal expansion process. On the other hand, higher vibration modes behave like springs at lower excitation frequencies; therefore, these omitted higher modes of the bladed-disk system can be represented by contact stiffnesses, which makes it possible to capture local deformations on the contact interface.

In the bladed-disk system with wedge dampers, dampers are initially not in contact with the blades. When the engine starts rotation due to the centrifugal effects, dampers come into contact with the neighboring blades. In order to include this effect, a normal force is assumed to act on the damper which presses it

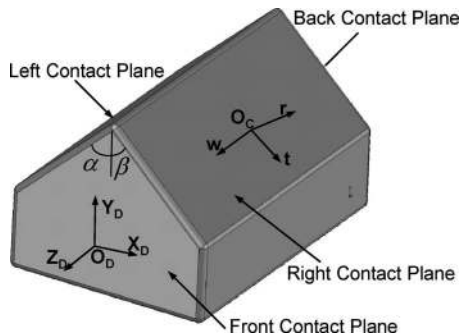


Fig. 3 Wedge damper contact planes and coordinate systems

against the adjacent blades. Therefore, for a static contact analysis, where the only force acting on the bladed-disk system is the normal force, the displacement at any contact point on the blade from modal analysis can be calculated by

$$\tilde{U}_B^i = - \sum_{j=1}^{n_C} \mathbf{R}_B^{i,j} {}^B F_j \quad (1)$$

$\mathbf{R}_B$  is the blade receptance matrix between contact points,  ${}^B F$  is the finite element contact force vector on the damper in the blade coordinate system, and  $n_C$  is the number of contact points. The difference in blade displacements with the finite element results can be expressed in the contact plane coordinate system as

$$\Delta U_B^i = {}^C U_B^i - {}^C \tilde{U}_B^i = {}^C U_B^i + \sum_{j=1}^{n_C} {}^C \mathbf{R}_B^{i,j} {}^C F_j \quad (2)$$

where  $\Delta U_B$  is the vector of difference in blade displacements, and  ${}^C \tilde{U}_B$  and  ${}^C U_B$  are the vectors of displacements from modal superposition and finite element contact analysis considering slip and separation at the contact pairs, respectively. Superscript  $C$  on the left of each parameter denotes the contact plane coordinate system. Blade residual stiffnesses at contact points are defined as

$$\mathbf{K}_{cB}^i \Delta U_B^i = - {}^C F_i \quad (3)$$

Substituting Eq. (2) in Eq. (3), the following relation is obtained:

$$\mathbf{K}_{cB}^{i-1} {}^C F_i = - \left( \sum_{j=1}^{n_C} {}^C \mathbf{R}_B^{i,j} {}^C F_j + {}^C U_B^i \right) \quad (4)$$

from which residual stiffnesses for the blade can be calculated.

The residual stiffness equation for the damper can be obtained similarly; however, the rigid body motion of the damper has to be considered. The displacements of contact points on the damper can be given in two parts,

$$\tilde{U}_D^i = \tilde{U}_{DR}^i + \tilde{U}_{DE}^i \quad (5)$$

where  $\tilde{U}_{DR}$  and  $\tilde{U}_{DE}$  are the vectors of rigid body and elastic damper displacements from modal analysis, and they are given as

$$\tilde{U}_{DR}^i = \Psi_i \boldsymbol{\eta} \quad (6)$$

$$\tilde{U}_{DE}^i = \sum_{j=1}^{n_C} \mathbf{R}_{DC}^{i,j} {}^D F_j + \sum_{j=1}^{n_P} \mathbf{R}_{DP}^{i,j} P_j \quad (7)$$

where  $\Psi_i$  is the rigid body mode shape matrix for the  $i$ th contact point,  $\boldsymbol{\eta}$  is the rigid body modal coefficient vector, and  $\mathbf{R}_{DC}$  and  $\mathbf{R}_{DP}$  are the receptance matrices between contact points and preload points, respectively.  ${}^D F$  and  $P$  are the vectors of contact forces and preloads acting on the damper in the damper coordinate system. Using Eqs. (6) and (7), the difference between modal superposition and finite element displacements in the contact plane coordinate system is obtained as

$$\Delta U_D^i = {}^C U_D^i - {}^C \tilde{U}_D^i = {}^C U_D^i - \left( {}^C \Psi_i \boldsymbol{\eta} + \sum_{j=1}^{n_C} {}^C \mathbf{R}_{DC}^{i,j} {}^C F_j + \sum_{j=1}^{n_P} {}^C \mathbf{R}_{DP}^{i,j} P_j \right) \quad (8)$$

The damper residual stiffness is defined as

$$\mathbf{K}_{cD}^i \Delta U_D^i = {}^C F_i \quad (9)$$

from which the following relation is obtained:

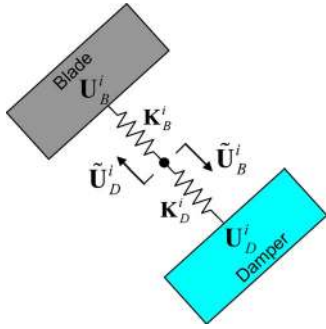


Fig. 4 Schematic view for the bounded configuration

$$\mathbf{K}_{cD}^{i-1} C F_i = C U_D^i - \left( C \Psi_i \eta + \sum_{j=1}^{n_C} C \mathbf{R}_{DC}^{ij} C F_j + \sum_{j=1}^{n_P} C \mathbf{R}_{DP}^{ij} P_j \right) \quad (10)$$

Assuming that the blade and damper contact pairs are bounded together, as shown in Fig. 4, the residual stiffness matrix for the  $i$ th contact pair can be written as follows:

$$\mathbf{K}_c^{i-1} = \mathbf{K}_{cB}^{-1} + \mathbf{K}_{cD}^{-1} \quad (11)$$

where  $\mathbf{K}_c^{i-1}$  is the residual stiffness matrix at the  $i$ th contact pair, which is referred to as contact stiffness matrix. It should be noted that in three-dimensional space there are nine unknowns in the residual stiffness matrix given in Eq. (11); hence, Eqs. (4) and (10) cannot be solved uniquely to determine these unknowns. However, if the residual stiffness matrix is assumed to be diagonal only, Eqs. (4) and (10) can be solved uniquely for the three unknowns on their diagonals. It can be concluded that the stiffnesses on the diagonal are in the three main directions of the contact plane coordinate system between blade and damper contact pairs. Since the friction model utilized is applied in the two major tangential directions, contact stiffnesses used in the developed friction model are in the three main directions; therefore, the assumption of the diagonal contact stiffness matrix is an appropriate one. Moreover, most of the friction models developed for the analysis of bladed-disk systems utilize diagonal contact stiffness matrices where off-diagonal coupling terms between tangential directions are used in the friction model given in Refs. [10,25], but to the best of the authors' knowledge, no friction model uses coupling between tangential and normal directions. Therefore, the method presented can be applied to other friction models as well.

### 3 Friction Contact Model and Forced Response Prediction

The relative motion at the blade-damper contact interface is three dimensional, and this relative motion is decomposed into in-plane and out-of-plane (normal) components. Furthermore, two major directions for the in-plane component of motion are determined, and the in-plane motion is approximated in these directions. Calculation of Fourier coefficients using a three-dimensional friction model as given in Ref. [10,25] is time consuming, and the main focus of this work is modeling damper motion as an unconstrained body having six degrees of freedom rigid body motion plus elastic motion. Therefore, in order to speed up the forced response calculations, these major directions are assumed to be independent of each other, and the one-dimensional friction model with normal load variation developed by Yang et al. [24] is employed. Transition criteria and analytical transition angles for harmonic motion are given in Ref. [24], and for periodic motion these criteria can be solved numerically to determine the transition angles. Therefore, the nonlinear normal force and the friction forces in major directions are obtained, which are then expressed in the contact plane coordinate system.

**3.1 Initial Preload on Contact Surfaces.** Depending on the engine rpm, the centrifugal force acting on the wedge dampers varies. This results in variation in the contact area and the preload/gap acting on the contact surfaces. In order to determine the initial preload/gap, a quasistatic contact analysis is performed for the given normal load. The analysis is performed as follows:

1. Initially, the contact status of all the contact pairs are assumed completely stuck.
2. The displacements of contact points and the contact forces acting on them are determined using the given contact status.
3. Using the Coulomb friction model, the contact status of each contact pair is updated.
4. The contact status of each contact pair is compared with previous contact status.
5. If the contact status is changed, go to step 2.
6. Otherwise, output the initial preload.

This analysis is an important step for the forced response calculations since the change of contact area and the preload/gap can affect the entire forced response characteristics of the blade and damper system. In order to increase the robustness of the method presented, a continuation method can be employed where the normal load is modified with a load factor between 0 and 1. Starting with a very low value, where the entire contact interface is completely stuck or very close to completely stuck, and applying the procedure given above, the contact state for this load step can be determined. The contact state for an increased load factor can be obtained by repeating the procedure given above where the previous solution is used as an initial guess at step 1. For the preload considered, the contact state and normal load acting on the contact interface will be obtained when the load factor reaches 1.

**3.2 Forced Response Method.** In the forced response analysis, finite element models for the blade (disk) and the damper are employed. Using receptance methods, the number of unknowns in the forced response analysis method can be decreased to the number of nonlinear (contact points) degrees of freedom multiplied by the number of harmonics. However, if the number of contact points is high, which is necessary for an accurate modeling of friction contact, this method is not suitable for forced response analysis due to large matrices involved in the solution procedure. Recently, Cigeroglu et al. [27] proposed a modal superposition method for the forced response analysis of bladed-disk systems. In this approach, the relative motion between contact surfaces is approximated by modal superposition using free mode shapes of the structure. This method is extended for multiple harmonics and is employed in this work. In the modal superposition approach, the number of unknowns involved in the solution procedure is the number of mode shapes used in the modal expansion process multiplied by the number of harmonics; therefore, it is independent of the number of contact points used. As a result of this, the modal superposition approach is suitable for accurate modeling of friction contact with more contact points or for cases when the tuned approach (cyclic symmetry) cannot be used.

The equation of motion in matrix form for a system with dry friction dampers can be written in the following form:

$$\mathbf{M} \cdot \ddot{X} + \mathbf{C} \cdot \dot{X} + \mathbf{K} \cdot X = F_e(t) + F_n(X) \quad (12)$$

where  $\mathbf{M}$ ,  $\mathbf{C}$ ,  $\mathbf{K}$ ,  $F_e(t)$ ,  $F_n(X)$ , and  $X$  are the mass matrix, viscous damping matrix, stiffness matrix, excitation force vector, nonlinear force vector, and displacement vector, respectively. The motion of the blade and the damper for harmonic excitation can be written in terms of its mode shapes as follows:

$$\mathbf{u}_B^j = \sum_{n=1}^{n_B} \mathbf{A}_{n,0} \phi_j^n + \sum_{l=1}^{n_H} \text{Im} \left( \sum_{n=1}^{n_B} \mathbf{A}_{n,l} \phi_j^n e^{j(l\theta)} \right)$$

$$\mathbf{u}_D^j = \sum_{n=1}^{n_R} \mathbf{C}_{n,0} \boldsymbol{\psi}_j^n + \sum_{n=1}^{n_E} \mathbf{D}_{n,0} \boldsymbol{\Phi}_j^n + \sum_{l=1}^{n_H} \text{Im} \left[ \left( \sum_{n=1}^{n_R} \mathbf{C}_{n,l} \boldsymbol{\psi}_j^n + \sum_{n=1}^{n_E} \mathbf{D}_{n,l} \boldsymbol{\Phi}_j^n \right) e^{i(l\theta)} \right] \quad (13)$$

where  $\boldsymbol{\phi}_j^n$ ,  $\boldsymbol{\psi}_j^n$ , and  $\boldsymbol{\Phi}_j^n$  are the  $n$ th mode shape vector for the  $j$ th blade node,  $n$ th rigid body mode shape, and elastic mode shape for the  $j$ th damper node, respectively.  $A_n^l$ ,  $C_n^l$ , and  $D_n^l$  are the  $l$ th harmonic modal coefficients for the blade, damper rigid body modes, and elastic modes, respectively, where  $l=0$  defines the bias terms.  $n_B$ ,  $n_R$ ,  $n_E$ , and  $n_H$  are the number of blade modes, damper rigid body modes, damper elastic modes, and harmonics, respectively. In addition to this,  $i$  is the imaginary unit and  $\theta$  is the temporal variable. The relative motion between the  $j$ th contact pair can be written in contact plane coordinates as

$$\Delta X_j = {}^C \mathbf{u}_B^j - {}^C \mathbf{u}_D^j = {}^C \mathbf{T}_j \cdot \mathbf{u}_B^j - {}^C \mathbf{T}_j \cdot \mathbf{u}_D^j \quad (14)$$

where  ${}^C \mathbf{T}_j$  and  ${}^D \mathbf{T}_j$  are the transfer matrices from the blade coordinate system to contact plane coordinates and from the damper coordinate system to contact plane coordinates for contact point  $j$ , respectively. Using the friction contact model and the relative motion given in Eq. (14), nonlinear contact forces can be determined in contact plane coordinates as

$${}^C F_n(\mathbf{A}, \mathbf{C}, \mathbf{D}, \theta) \equiv {}^C F_n^0(\mathbf{A}, \mathbf{C}, \mathbf{D}) + \sum_{l=1}^{n_H} {}^C F_{ns}^l(\mathbf{A}, \mathbf{C}, \mathbf{D}) \sin(l\theta) + \sum_{l=1}^{n_H} {}^C F_{nc}^l(\mathbf{A}, \mathbf{C}, \mathbf{D}) \cos(l\theta) \quad (15)$$

where  ${}^C F_n^0$  is the bias term of vector of contact forces and,  ${}^C F_{ns}^l$  and  ${}^C F_{nc}^l$  are the vectors of sine and cosine components of the  $l$ th harmonic of contact forces, which are functions of modal coefficients  $\mathbf{A}$ ,  $\mathbf{C}$ , and  $\mathbf{D}$ . Using the orthogonality of mode shapes and Eq. (15), Eq. (12) for a single sector can be written in the following form:

$$\begin{aligned} \boldsymbol{\Omega}_B \mathbf{A}^{(0)} &= \mathbf{Q}_{B_b}^0 \\ (\boldsymbol{\Omega}_B - (l\omega)^2 \mathbf{I} + i(l\omega) \mathbf{C}_B) \mathbf{A}^{(l)} &= \mathbf{Q}_e^l + \mathbf{Q}_{B_{Re}}^l + i \mathbf{Q}_{B_{Im}}^l \\ 0 &= {}_j \mathbf{Q}_{D_b}^0 \quad (j = 1 \cdots n_R) \\ \boldsymbol{\Omega}_D^j \mathbf{D}_{j,0} &= {}_j \mathbf{Q}_{D_b}^0 \quad (j = n_R + 1 \cdots n_D = n_R + n_E) \\ (\boldsymbol{\Omega}_D - (l\omega)^2 \mathbf{I} + i(l\omega) \mathbf{C}_D) \mathbf{E}^{(l)} &= \mathbf{Q}_{D_{Re}}^l + i \mathbf{Q}_{D_{Im}}^l \quad (l = 1 \cdots n_H) \end{aligned} \quad (16)$$

if mass normalized mode shapes are used. In Eq. (16),  $\boldsymbol{\Omega}_B$  and  $\boldsymbol{\Omega}_D$  are  $n_B \times n_B$  and  $n_D \times n_D$  diagonal matrices of squares of natural frequencies of the blade and the damper.  $\mathbf{C}_B$  and  $\mathbf{C}_D$  are modal damping matrices of the blade and the damper, and they are diagonal if the damping is proportional.  $\mathbf{A}^{(l)}$  is the vector of modal coefficients of the blade, and  $\mathbf{E}^{(l)}$  is the vector of modal coefficients of the damper for the  $l$ th harmonic, which is composed of rigid body and elastic mode shapes as  $\mathbf{E} = (\mathbf{C} \ \mathbf{D})^T$ .  $\mathbf{Q}_e^l$  and  $\mathbf{Q}_D^l$  are the vectors of modal forces of the  $l$ th harmonic for the blade and damper, respectively, and  $e$ ,  $b$ ,  $Re$ , and  $Im$  stand for excitation force, bias component, real part, and imaginary part, respectively. It should be noted that the contact forces acting on the  $j$ th blade and the  $j$ th damper in contact plane coordinate system are the same in magnitude but opposite in signs. If the bladed-disk system is tuned due to the cyclic symmetry, the motion of the  $(j+1)$ th blade can be related to the motion of the  $j$ th blade as

$$\mathbf{u}_B^{j+1}(\theta) = \mathbf{u}_B^j(\theta + \varphi), \quad \varphi = 2\pi n_{EO}/n_b \quad (17)$$

where  $\varphi$  is the interblade phase angle,  $n_{EO}$  is the engine order, and  $n_b$  is the number of blades. Using this information, the relative displacement on the contact surfaces of the  $j$ th damper can be determined, from which contact forces acting on the  $j$ th damper can be obtained. Similar to the displacements, contact forces between the  $(j-1)$ th damper and  $j$ th blade can be related as

$$F_n^j(\theta) = F_n^{j+1}(\theta - \varphi) \quad (18)$$

where  $F_n^j$  is the nonlinear contact forces acting on the  $j$ th blade in the blade coordinate system. Transferring contact forces between the  $j$ th damper and the  $(j-1)$ th blade to the  $j$ th blade, the modal coefficients of the  $j$ th blade and damper can be determined by iteratively solving the nonlinear equation set given in Eq. (16); consequently, the blade and damper responses can be obtained from Eq. (13).

## 4 Numerical Results

Two different cases are analyzed in this section. In the first part, the method is applied to a tuned bladed-disk system, and forced response curves and optimal curves are presented. Moreover, the effects of normal load on the rigid body coefficients of the damper and the effects of rotational motion of the damper on the forced response results are studied. In order to show the effect of partial slip on the forced response analysis, the bladed-disk system is analyzed for different numbers of contact points. In the second part, a blade-to-ground damper system is analyzed in order to show the effects of multiharmonics on the forced response. In the results provided below, stuck case indicates that all the contact points that are initially in contact do not slip. Therefore, it is possible to have contact points, which are not in contact due to the applied normal load. These are identified in the quasistatic contact analysis.

**4.1 Tuned Bladed-Disk System With Wedge Dampers.** A tuned bladed-disk system with wedge dampers, composed of 65 blades and dampers, is studied in this part. Finite element models of a blade and a damper are given in Fig. 5. The point of excitation and the point where displacement is calculated are indicated by dots, as shown in the figure. In the analysis, fifth engine order excitation is considered, and ten modes for the blade and six rigid body modes for the damper are used. In the forced response calculations only the fundamental harmonic is kept due to reasons that will be explained in Sec. 4.2.

**4.1.1 Forced Response and Optimal Curves.** Tracking plots around the first and second modes of the blade are given in Figs. 6 and 7 for different preload cases. External force applied at the tip point is in the tangential direction for the first mode and in the radial direction for the second mode in order to excite those modes. It is observed that as the preload acting on the damper increases, the amplitude of tip point displacement decreases and the resonance frequency of the system increases. When the optimum point is reached, the amplitude is minimum, and increasing the preload further results in an increase in the vibration amplitude, which converges to the completely stuck magnitude. It is interesting to note that in Fig. 6 multiple solutions in the tracking plots exist for some preload cases, whereas in Fig. 7 none of the preload cases results in multiple solutions in the tracking plots. These multiple solutions are due to the separation of the contact surfaces. In Fig. 6, the first bending mode of the blade is excited, resulting in the separation of the contact surfaces due to the rotation of the wedge damper about the  $Z$  axis. However, in Fig. 7, since the dominant rotation is about the  $X$  axis, contact surfaces remain in contact throughout the analysis. Multiple solutions in the tracking plots are obtained by the continuation method, and they show a typical fold bifurcation, which has an unstable solution branch in between two stable solutions resulting in the jump

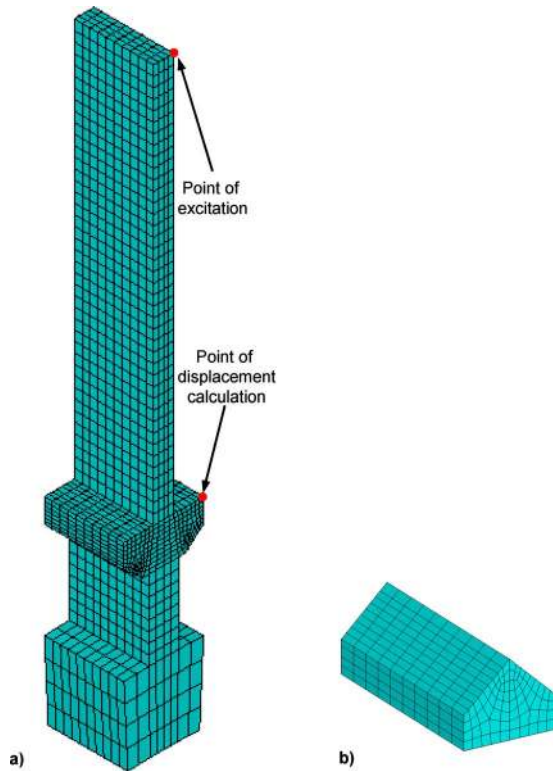


Fig. 5 Finite element models for (a) blade and (b) wedge dampers

phenomenon.

In Figs. 8 and 9, optimal curves and frequency shift curves for the first and second vibration modes of the blade are given. It is observed that the ratio of the stuck case amplitude to the optimal preload case amplitude is approximately 4.4 and 5.5 for the first and second modes of vibration, respectively. Due to the fact that there exists no separation between the wedge damper and the adjacent blades, damping at the second mode is more effective. However, since the decrease in the free response amplitude at the first mode is larger than the second mode, damper works more effectively at the first mode. The frequency shifts observed for the first and second modes are 17.2% and 3.4%, respectively.

Using the computer code (BDAMPER) developed for the analysis of bladed-disk systems with wedge dampers, higher modes of the

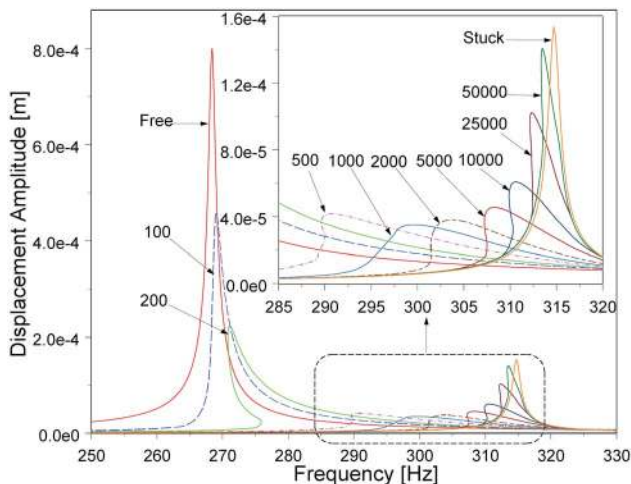


Fig. 6 Tracking plot for the first mode

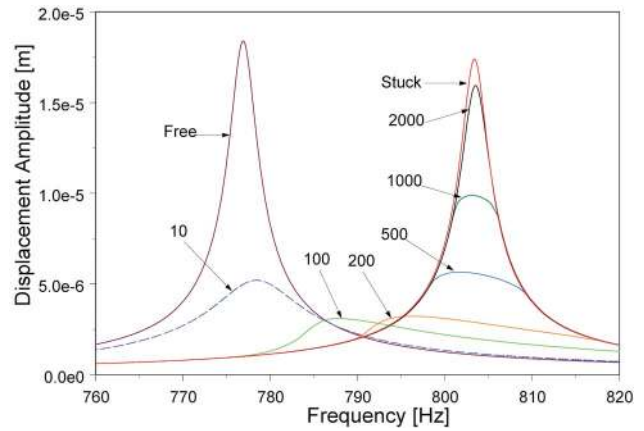


Fig. 7 Tracking plot for the second mode

blade can also be investigated. The tracking plots and optimum and frequency shift curves for the third and seventh modes of the blade are given in Figs. 10 and 11.

4.1.2 Effects of Normal Load and Excitation Frequency on Rigid Body Motion. In Figs. 12 and 13, maximum amplitudes of the bias and vibratory components of rigid body modal coefficients of the wedge damper are given for the first vibration mode, respectively. For low normal load cases, modal coefficients for translation along  $X$  and  $Y$  axes and for rotation about the  $Z$  axis

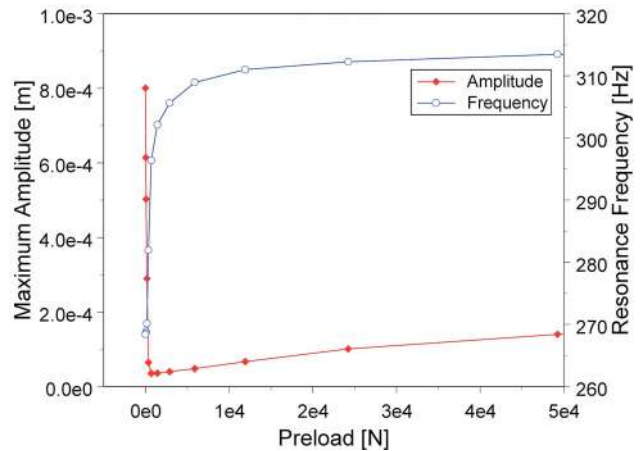


Fig. 8 Optimal and frequency shift curves: first mode

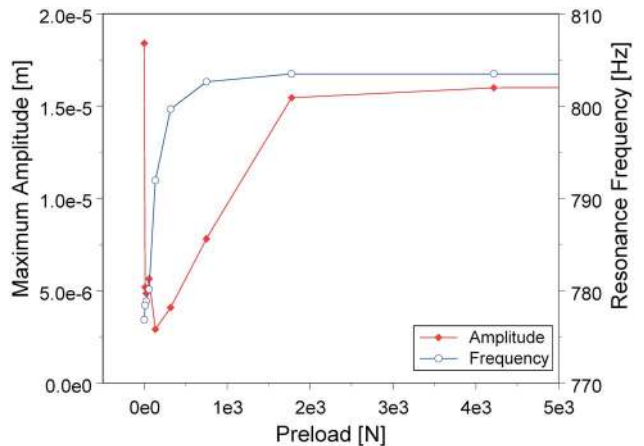


Fig. 9 Optimal and frequency shift curves: second mode

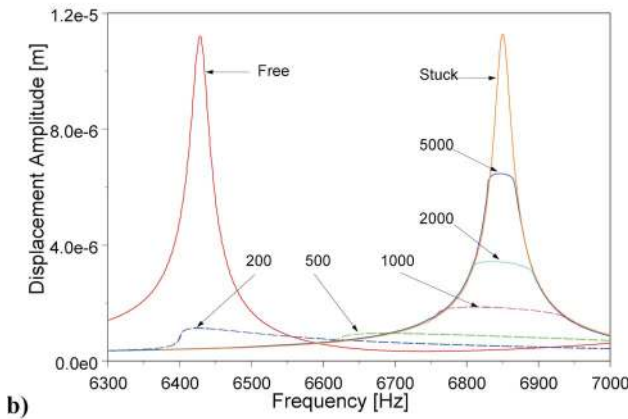
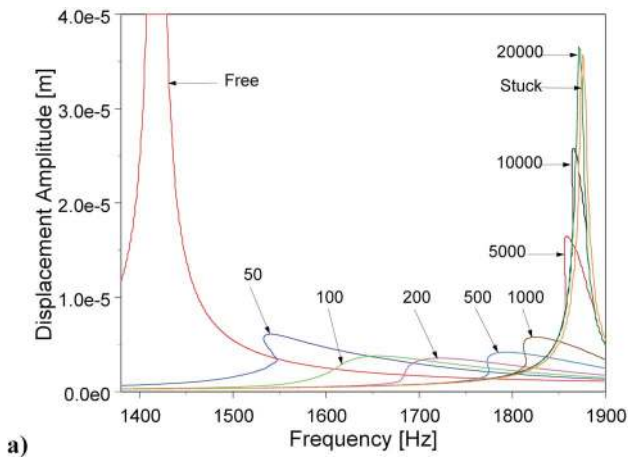
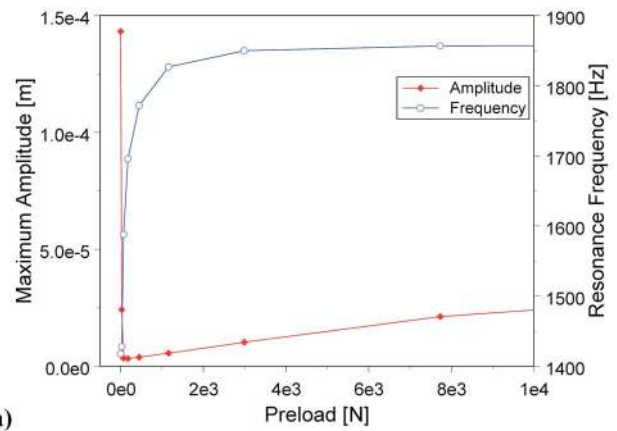


Fig. 10 Tracking plots: (a) third and seventh (b) modes

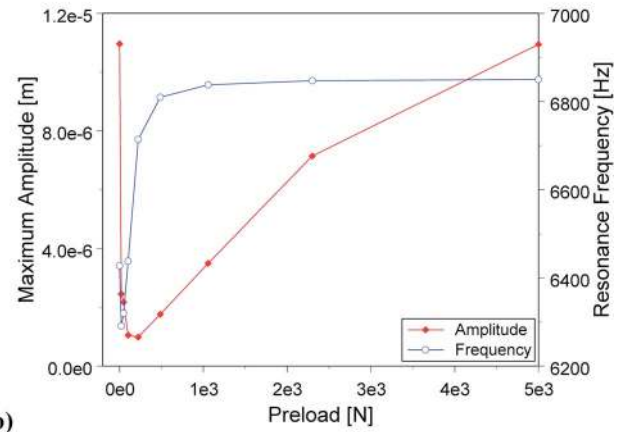
are the main contributions to the damper rigid body motion, and as the normal load increases, the major contribution comes from the modal coefficient for translation along the  $Y$  axis. Similarly, the major variable components of rigid body motion are translation along  $X$  and  $Y$  axes and rotation about the  $Z$  axis. For all normal load ranges, major variable components of rigid body motion are in the order of translation along  $X$ , rotation about  $Z$ , and translation along  $Y$ . It should be noted that rotation of the damper about the  $Z$  axis results in the separation of the contact surfaces, which results in multiple solutions or jumps in the tracking plots.

The bladed-disk system is analyzed using only the translational rigid body modes and translational and rotational rigid body modes of the damper at the first vibration mode of the blade. The results, including and excluding the rotational modes for different normal load cases, are compared in Fig. 14. It is observed that neglecting the rotation of the damper results in an underestimation of the maximum vibration amplitudes; in addition to this, frequency shift is overestimated for this case. It is also interesting to note that a jump phenomenon (multiple solutions) does not exist if the rotational modes of the damper are neglected. Therefore, it can be concluded that the separation of the contact surfaces is associated with the rotation of the damper.

**4.1.3 Effects of Partial Slip on Forced Response.** In order to observe the effects of partial slip, the forced response analysis is performed for different numbers of contact points on the left and right contact planes. Figure 15 shows the comparison of forced response results for different normal load cases for  $9 \times 9$ ,  $24 \times 24$ , and  $48 \times 48$  contact points. It is observed that multiple solutions in the forced response are captured better when more contact points are employed in the analysis. Moreover, using  $9 \times 9$  contact points resulted in an underestimation of the vibration am-



a)



b)

Fig. 11 Optimum and frequency shift curves: (a) third and seventh (b) mode

plitude in the cases studied. The results for  $24 \times 24$  and  $48 \times 48$  contact points are closer to each other,  $48 \times 48$  having the highest vibration amplitude in most of the cases. However, employing more contact nodes results in longer calculation times; therefore, optimum values for the number of contact points can be determined by comparing the forced response results.

In Fig. 16, the contact status of four sample contact points on the left and right contact planes of the wedge damper are shown

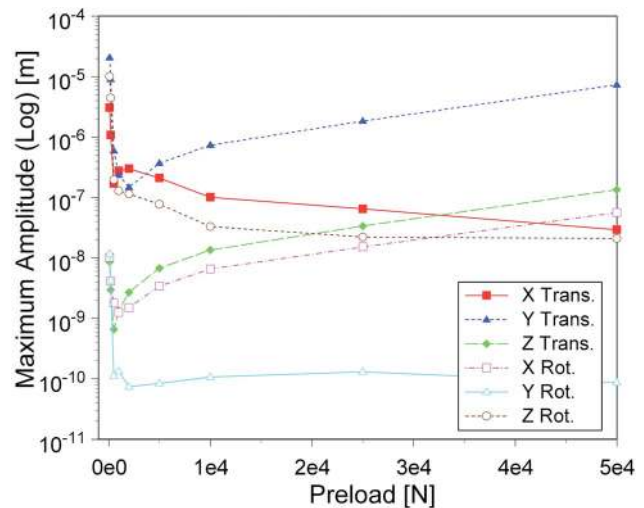


Fig. 12 Effect of normal load on the rigid body motion of damper (bias component)

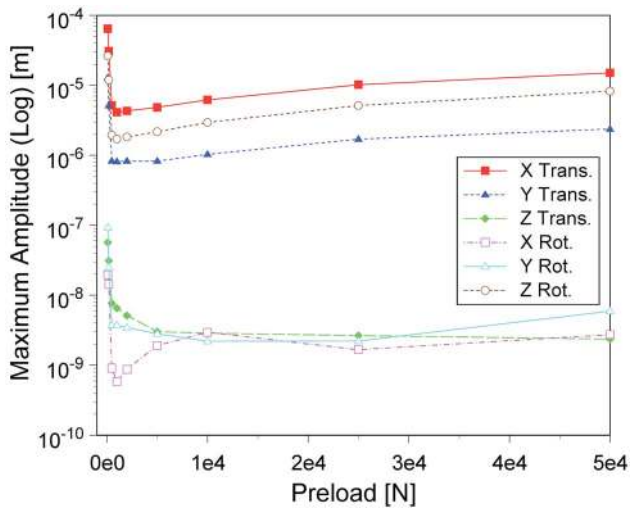


Fig. 13 Effect of normal load on the rigid body motion of damper (vibratory component)

for the normal load of 5000 N at the maximum amplitude frequency of 308.3 Hz. The length of the bar represents the periodic temporal scale. Partial slip on both contact surfaces can be clearly seen from the figure where contact points undergo different states at different times.

#### 4.2 Blade-to-Ground Damper System

**4.2.1 Effect of the Number of Harmonics on the Forced Response.** In order to present the effect of the number of harmonics on the forced response of frictionally constrained structures, a blade-to-ground damper system is investigated, where the blade given in Fig. 5 is in contact with the ground from the right side, as shown in Fig. 17. This simple model is chosen in order to decrease the number of unknowns and hence decrease the computational time for the analysis as well as to control the initial preload/gap distribution, as requested.

Tracking plots for the blade-to-ground damper system are given in Fig. 18 for single-harmonic and multiple-harmonic responses. It is observed that for the cases where multiple solutions exist, the difference between the single- and multiple-harmonic solutions is is

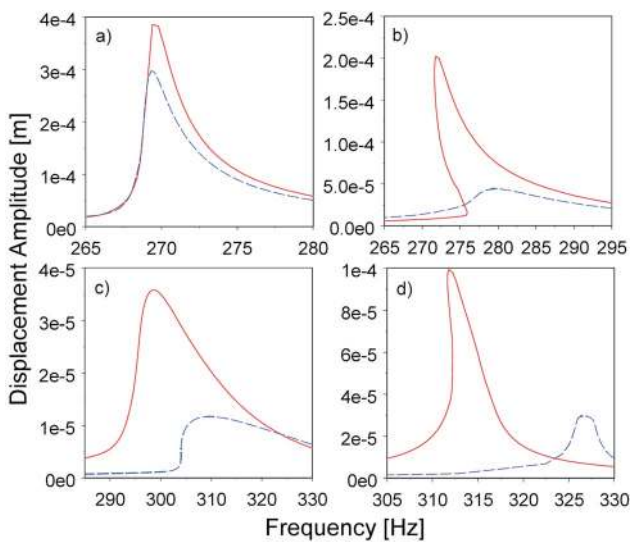


Fig. 14 Effect of rotational modes for normal load; (a) 100, (b) 200, (c) 1000, and (d) 10,000; —, translational and rotational modes; -----, translational modes

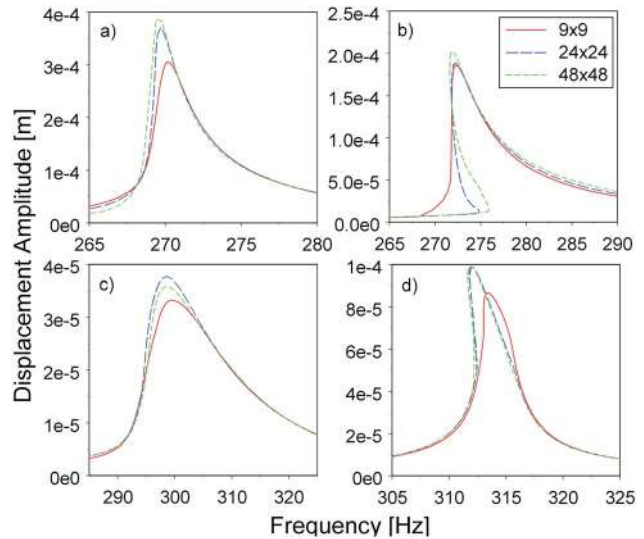


Fig. 15 Effect of the number of contact points for normal load; (a) 100, (b) 200, (c) 1000, and (d) 25,000

significant. This is due to the separation of the contact interface, and it can be concluded that, if separation occurs single-harmonic solution cannot capture the nonlinear characteristics accurately. However, for high preload cases, a single-harmonic solution cap-

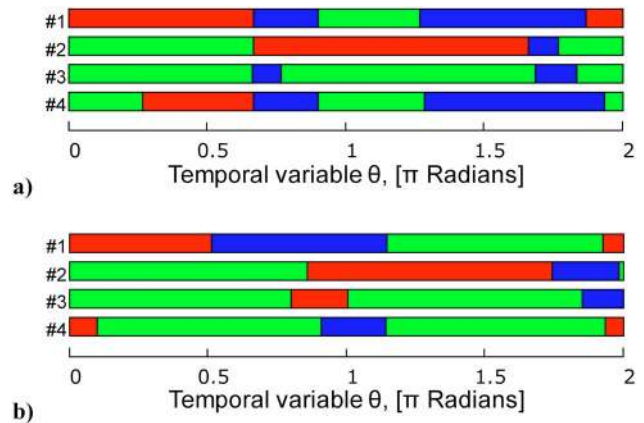


Fig. 16 Contact status of sample points on (a) left (b) right contact planes: (red) stick, (blue) slip, and (green) separation). (Color version of this figure available online only.)

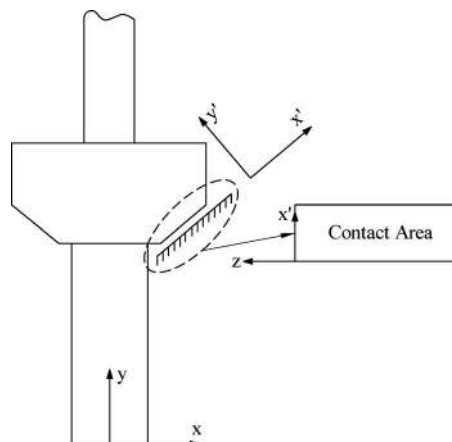
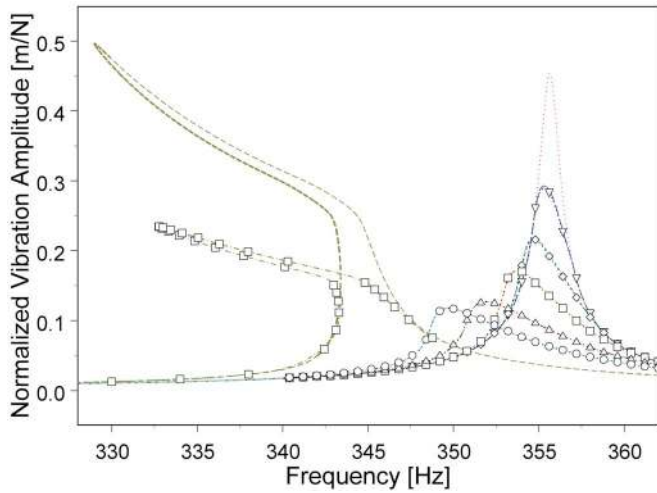


Fig. 17 Schematic for the blade to ground damper





**Fig. 18 Tracking plots, (.....), stuck; single-harmonic: (— — —) 1.0e6, (-----) 5.0e5, (--- --) 2.5e5, (-·-·-·) 1.0e5, (— · — ·) 5.0e4, (--- · ---) 1.0e4; multiharmonic: (· · ∇ · ·) 1.0e6, (· · ◇ · ·) 5.0e5, (· · □ · ·) 2.5e5, (· · △ · ·) 1.0e5, (· · ○ · ·) 5.0e4, and (- - □ - -) 1.0e4**

tures the nonlinear characteristics quite well and the difference between the single- and multiple-harmonic solutions is negligible. This result is also in agreement with the findings of Chen and Menq [10].

**4.3 Comparison With the Test Case Data.** In order to verify the developed method, prediction for a test blade, used by GE aircraft engines in a friction damping experiment, is compared with the test data. The schematic for the experimental setup is given in Fig. 19, where two wedge dampers are placed at each side of the test blade, and they are retained by two dummy blades without any airfoils. The normal load on the damper is adjusted by controlling the tension in the damper load wires. The test blade is excited by a pulsating air jet, where the excitation levels are controlled by air-jet supply pressure. Strain gages are placed at several locations on the blade, including the airfoil root, in order to measure the vibratory stresses.

The finite element model of the test case is given in Fig. 20. Since the developed computer code is designed for a tuned system analysis, the test blade and the dummy blades are considered as a single structure for which the interblade phase angle is zero. A comparison of the predicted frequency shift curve with the available test data is given in Fig. 21. For high damper load cases, predicted frequency shift is lower than the test data. However, overall, the predicted frequency shift curve is in good agreement with the experimental data. It should be noted that these predic-

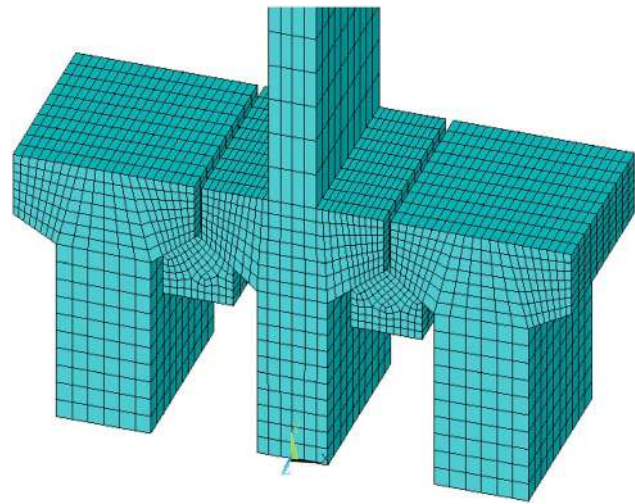


**Fig. 20 Finite element model for the test case**

tions are done by using the contact stiffnesses calculated by the proposed approach, as discussed previously. In Fig. 22, the predicted normalized optimal curve and the test data are presented. It is observed that predictions and test results are in good agreement, and the optimal damper load can be predicted acceptably without any parameter tuning. The only parameter to be determined is the friction coefficient, which, in this case, was acquired experimentally. Due to the acyclic structure of the test case, complete locking of the contact surfaces is not possible, which results in mi-

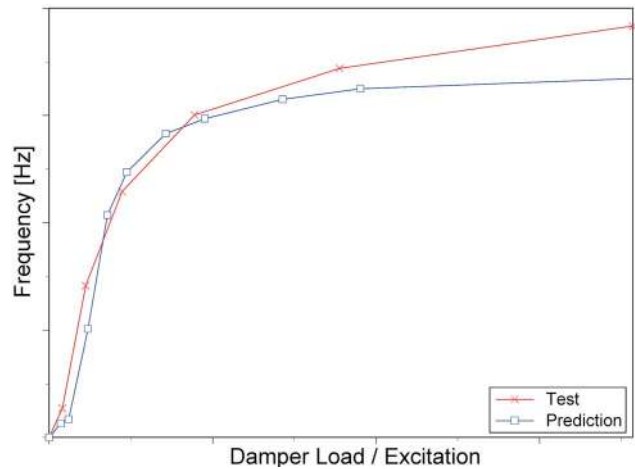


**Fig. 21 Frequency shift curve**

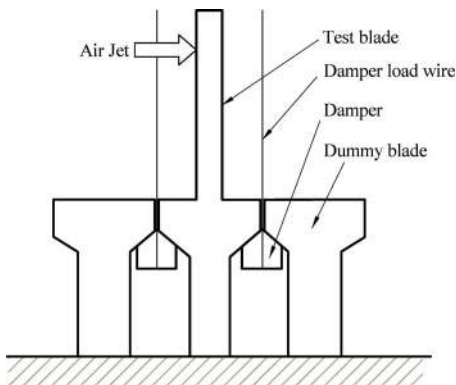


**Fig. 19 Schematic view of the test case**

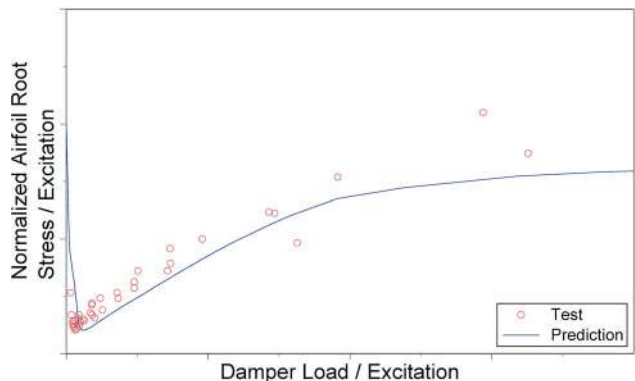


**Fig. 22 Predicted normalized optimal curve and test data**

crosslip for those cases. This can clearly be seen from the predictions given in Fig. 22. Predictions for the test case are also performed for including more blade modes into the analysis, for which contact stiffnesses are recalculated, and it is observed that predictions obtained from both cases are similar and very close to each other. All these results are not presented here for brevity.

## 5 Conclusions

A forced response prediction method for the analysis of constrained and unconstrained structures coupled through frictional contacts is presented. In the developed method, the unconstrained structure is modeled as a solid body having six rigid body motions as well as elastic deformation. Discrete contact points, which are associated with contact stiffnesses in three directions of motion, are distributed on the contact surfaces. In order to determine the initial preload or gap at each contact point, a quasistatic contact analysis is performed initially for each normal load acting on the damper.

A method is proposed to calculate the contact stiffnesses used in the friction model. The suggested method is based on representing the effect of higher vibration modes by springs associated with each contact pair, which makes it possible to capture local deformations at the contact interface. Therefore, contact kinematics can be accurately estimated by using a reasonable number of mode shapes in the forced response prediction, which decreases the computational cost significantly.

For the forced response analysis, a friction model with normal load variation induced by normal motion is employed to determine the three dimensional contact forces. The harmonic balance method is employed to approximate these contact forces in order to calculate the forced response of constrained and unconstrained structures coupled through frictional contacts. Modal superposition is used to express the relative motion; therefore, the number of unknowns in the resulting nonlinear equation set is proportional to the number of modes and the number of harmonics employed in the analysis, and it is independent of the number of contact points.

The developed forced response prediction method is demonstrated on an example bladed-disk system with wedge dampers, where blades and dampers represent the constrained and unconstrained structures, respectively. A tuned bladed-disk system is studied by the method developed, and forced response results are presented. Multiple solutions (jumps) in the tracking plots for the first vibration mode are observed, which are due to the separation of the contact surfaces associated with the rotation of the damper about the  $Z$  axis.

For the first vibration mode, the major contributions to the vibratory component of motion comes from the translation along the  $X$  axis, rotation about the  $Z$  axis, and translation along the  $Y$  axis. In addition to this, the effects of rotational modes are also analyzed, and it is observed that neglecting rotational modes results in an underestimation of the vibration amplitude and an overestimation of the frequency shift. Moreover, no multiple solutions (jumps) in the tracking plots are observed if the rotational modes are neglected.

In order to analyze the effects of partial slip, forced response predictions are calculated for three different numbers of contact points. Utilizing more contact points makes it possible to capture the stick-slip-separation phenomenon of the contact surfaces more accurately, which is observed in contact status plots. The method developed can be used to obtain optimum values for the number of contact points in order to meet the accuracy and computational requirements.

The effects of multiple harmonics are also investigated on a blade-to-ground damper example. It is observed that multiple harmonics is necessary only for the case of jump, where the normal load is low; on the other hand, for high normal loads, multiple harmonics and single-harmonic solutions are approximately the

same. Since friction dampers are designed to work at higher damper loads, single-harmonic solutions will be adequate for damper optimization purposes.

Finally, predictions for a test case are compared with the test data, and it is observed that simulation results and test results are in good agreement. Similar forced response predictions are obtained by increasing the number of blade modes used in the analysis, which verifies the developed forced response prediction method and contact stiffness calculation method presented. Utilizing the contact stiffnesses obtained by the proposed method, parameter tuning for contact stiffnesses is eliminated, and the only contact parameter left to be determined is the friction coefficient, which significantly simplifies the forced response prediction process.

## Acknowledgment

This material is based on work supported by the Guide Consortium of the Carnegie-Mellon University, which is sponsored by the Air Force Research Laboratory under Contract No. F33615-01-C-2186. The Consortium director is Professor Jerry H. Griffin.

## References

- [1] Yang, B. D., and Menq, C. H., 1998, "Characterization of Contact Kinematics and Application to the Design of Wedge Dampers in Turbomachinery Blading: Part 1—Stick-Slip Contact Kinematics," *ASME J. Eng. Gas Turbines Power*, **120**, pp. 410–417.
- [2] Yang, B. D., and Menq, C. H., 1998, "Characterization of Contact Kinematics and Application to the Design of Wedge Dampers in Turbomachinery Blading: Part 2—Prediction of Forced Response and Experimental Verification," *ASME J. Eng. Gas Turbines Power*, **120**, pp. 418–423.
- [3] Sanliturk, K. Y., Ewins, D. J., and Stanbridge, A. B., 2001, "Underplatform Dampers for Turbine Blades: Theoretical Modeling, Analysis, and Comparison With Experimental Data," *ASME J. Eng. Gas Turbines Power*, **123**, pp. 919–929.
- [4] Pfeiffer, F., and Hayek, M., 1992, "Stick-Slip Motion of Turbine Blade Dampers," *Philos. Trans. R. Soc. London, Ser. A*, **338**, pp. 503–517.
- [5] Sextro, W., Popp, K., and Walter, T., 1997, "Improved Reliability of Bladed-Disks to Friction Dampers," *ASME International Gas Turbine and Aeroengine Congress and Exposition*, Orlando, June.
- [6] Csaba, G., 1999, "Modeling of a Microslip Friction Damper Subjected to Translation and Rotation," *ASME International Gas Turbine Conference*, Indianapolis, June.
- [7] Jareland, M. H., 2001, "Experimental Investigation of a Platform Damper With Curved Contact Areas," *ASME Design Engineering Conference*, Pittsburgh.
- [8] Panning, L., Sextro, W., and Popp, K., 2003, "Spatial Dynamics of Tuned and Mistuned Bladed-Disks With Cylindrical and Wedge-Shaped Friction Dampers," *Int. J. Rotating Mach.*, **9**, pp. 219–228.
- [9] Menq, C. H., Griffin, J. H., and Bielak, J., 1986, "The Forced Response of Shrouded Fan Stages," *ASME J. Vib., Acoust., Stress, Reliab. Des.*, **108**, pp. 50–55.
- [10] Chen, J. J., and Menq, C. H., 2001, "Periodic Response of Blades Having Three-Dimensional Nonlinear Shroud Constraints," *ASME J. Eng. Gas Turbines Power*, **123**, pp. 901–909.
- [11] Ferrero, J. F., Yettou, E., Barrau, J. J., and Rivallant, S., 2004, "Analysis of a Dry Friction Problem Under Small Displacements Application to a Bolted Joint," *Wear*, **256**, pp. 1135–1143.
- [12] Quin, D. D., and Segalman, D. J., 2005, "Using Series-Series Iwan-Type Models For Understanding Joint Dynamics," *ASME J. Appl. Mech.*, **72**, pp. 666–673.
- [13] Ouyang, H., Oldfield, M. J., and Mottershead, J. E., 2006, "Experimental and Theoretical Studies of a Bolted Joint Excited by a Torsional Dynamic Load," *Int. J. Mech. Sci.*, **48**, 1447–1455.
- [14] Padmanabhan, C., 1994, "Analysis of Periodically Excited Systems With Clearances," Ph.D. thesis, The Ohio State University.
- [15] Duan, C., and Singh, R., 2005, "Transient Responses of a 2-DOF Torsional System With Nonlinear Dry Friction Under a Harmonically Varying Normal Load," *J. Sound Vib.*, **285**, pp. 1223–1234.
- [16] Duan, C., and Singh, R., 2006, "Dynamics of a 3DOF Torsional System With a Dry Friction Controlled Path," *J. Sound Vib.*, **289**, pp. 657–688.
- [17] Griffin, J. H., 1980, "Friction Damping of Resonant Stresses in Gas Turbine Engine Airfoils," *ASME J. Eng. Power*, **102**, 329–333.
- [18] Dowell, E. H., and Schwartz, H. B., 1983, "Forced Response of a Cantilever Beam With a Dry Friction Damper Attached, Part I: Theory," *J. Sound Vib.*, **91**, pp. 255–267.
- [19] Cameron, T. M., Griffin, J. H., Kielb, R. E., and Hoosac, T. M., 1990, "An Integrated Approach for Friction Damper Design," *ASME J. Vib. Acoust.*, **112**, pp. 175–182.
- [20] Ferri, A. A., 1996, "Friction Damping and Isolation Systems," *ASME J. Vib. Acoust.*, **117**(B), pp. 196–206.
- [21] Cigeroglu, E., Lu, W., and Menq, C. H., 2006, "One-Dimensional Dynamic

- Microslip Friction Model,” *J. Sound Vib.*, **292**, pp. 881–898.
- [22] Sanliturk, K. Y., and Ewins, D. J., 1996, “Modeling Two-Dimensional Friction Contact and Its Application Using Harmonic Balance Method,” *J. Sound Vib.*, **193**, pp. 511–523.
- [23] Menq, C. H., and Yang, B. D., 1998, “Non-Linear Spring Resistance and Friction Damping of Frictional Constraints Having Two-Dimensional Motion,” *J. Sound Vib.*, **217**, pp. 127–143.
- [24] Yang, B. D., Chu, M. L., and Menq, C. H., 1998, “Stick-Slip-Separation Analysis and Non-Linear Stiffness and Damping Characterization of Friction Contacts Having Variable Normal Load,” *J. Sound Vib.*, **210**, pp. 461–481.
- [25] Yang, B. D., and Menq, C. H., 1998, “Characterization of 3D Contact Kinematics and Prediction of Resonant Response of Structures Having 3D Frictional Constraint,” *J. Sound Vib.*, **217**, pp. 909–925.
- [26] Petrov, E. P., and Ewins, D. J., 2003, “Analytical Formulation of Friction Interface Elements for Analysis of Nonlinear Multi-Harmonic Vibrations of Bladed-Disks,” *ASME J. Turbomach.*, **125**, pp. 364–371.
- [27] Cigeroglu, E., and An, N., Menq, C. H., 2007, “A Microslip Friction Model With Normal Load Variation Induced by Normal Motion,” *Nonlinear Dyn.*, **50**(3), pp. 609–626.